

Role of the nonmagnetic layer in determining the Landé g -factor in a spin-transfer system

J.-S. Lee,¹ E. Vescovo,¹ C.-C. Kao,¹ J.-M. Beaujour,² A. D. Kent,² H. Jang,³ J.-Y. Kim,³ J.-H. Park,³ and J. H. Shim⁴

¹National Synchrotron Light Source, Brookhaven National Laboratory, Upton, New York 11973, USA

²Department of Physics, New York University, 4 Washington Place, New York, New York 10003, USA

³Department of Physics and PAL, Pohang University of Science and Technology, Pohang 790-784, South Korea

⁴Department of Chemistry, Pohang University of Science and Technology, Pohang 790-784, South Korea

(Received 18 September 2009; published 2 November 2009)

The microscopic origin of the Landé g -factor in two ferromagnetic/nonmagnetic (FM/NM) bilayer systems—Co/Cu and Ni/Pd—has been investigated using x-ray magnetic circular dichroism, resonant magnetic reflectivity, and band calculations. The FM/NM bilayer represents the building block of any complete spin-transfer structure (FM1/NM/FM2). The valence electronic structure is profoundly altered over a finite length across the FM/NM interface. A considerable charge transfer takes place from the NM to the FM material. This results in an enhancement of the orbital-to-spin magnetic moment ratio in the FM layer and an induced magnetic polarization in the NM layer. Both effects turn out to be crucial for a correct understanding of the g -factor in spin-transfer systems.

DOI: [10.1103/PhysRevB.80.180403](https://doi.org/10.1103/PhysRevB.80.180403)

PACS number(s): 75.47.-m, 75.70.-i, 85.75.-d

Substantial advances in information technology necessitate the development of ever smaller devices, while maintaining high-quality performance and high speed. In this context, great hope is placed on spin-based electronic devices and especially on those devices displaying the so-called spin-transfer mechanism,¹⁻³ a concept theoretically proposed by Slonczewski and Berger in 1996.^{4,5} Basically, spin-transfer phenomena occur whenever a spin-polarized current, originated in a ferromagnetic (FM)1, is forced to flow, via a nonmagnetic (NM) interlayer, into a second noncollinear FM2. Under proper size conditions, the forced change in angular momentum originates a torque capable of inducing dynamic precession phenomena in the macroscopic magnetization.^{6,7} On this basis, it has been possible to explain exotic phenomena such as spin precession of transversely polarized electrons⁸ or the behavior of the Gilbert damping constant,⁹ G . The quantitative determination of all factors controlling the critical currents for magnetization dynamics remains therefore a primary goal. Besides its intrinsic interest, the detailed understanding of the physics of spin transfer holds great promise to substantially advance spin technologies.¹⁰

The Landé g -factor and the closely related G constant have been mostly investigated in the FM-NM system,¹¹ and, a consistent enhancement of the g -factor by a few percent has been repeatedly observed compared to values of a single FM layer. Additionally, a characteristic inverse dependence of the g -factor on the FM layer's thickness has been reported in a variety of FM/NM systems, including NM layers of Cu, Pd, and Pt. These findings undoubtedly point toward an interface effect and are usually referred to as the anomalous g -factor. Significant anomalous contributions to spin precession and/or damping have been, for example, observed in Co/Cu, Co/Pt, Ni/Pd, Py(Ni₈₀Fe₂₀)/Pd, Py/Pt, and Py/Cu bilayer systems.^{12,13} Usually, this anomalous behavior is attributed to the increase of the orbital-to-spin moment ratio in the FM layer at the FM/NM interface.¹⁴ However, quantitative calculations based on this model consistently underestimate the observed g values, especially for relatively thick FM layers. In other instances, arguments based on the modification either of the spin diffusion length¹⁵ or of the Fermi surface¹⁶

at the FM/NM interface have been invoked to explain the anomalous g -behavior. However, these suggestions have never been pursued to a quantitative level.

In this work, we report on a microscopic investigation aimed at clarifying the role of the NM layer in determining the Landé g -factor in two FM/NM structures, Co/Cu and Ni/Pd. First, band calculations for these systems reveal a substantial charge transfer of $3d$ electrons upon formation of the FM-NM interface, profoundly modifying the magnetic moments in both the FM and the NM layer. Furthermore, the induced magnetization in the NM layer is found to be distributed over a finite thickness of a few Å inside the NM layer. Although the main contribution to the anomalous g -factor originates from the increase of the orbital-to-spin moment ratio in the FM layer, an additional contribution due to the finite magnetic thickness of the NM layer is necessary to correctly derive the g -factor in FM/NM structures. The role of the NM layer in determining the anomalous g -factor is therefore twofold: an indirect role, via a compounding of the moment ratio in the FM layer through charge transfer but also a direct role resulting from its own magnetization extending over a finite length from the interface.

As a first simplified structure representing a realistic spin-transfer system, we chose the following metallic multilayer: Ta/Co/Cu/Pt/GaAs [001]. We will refer to this system as the Co (3 nm)/Cu (3 nm) bilayer. The bilayer was sandwiched between a Pt (1.5 nm) layer, simulating a spin-sink to prevent spin back-flow from the outer edges and a Ta (1 nm) capping layer to minimize contamination effects. These samples were prepared by combination e -beam evaporation and sputtering under base pressure 5×10^{-8} Torr. X-ray magnetic circular dichroism (XMCD) and x-ray resonant magnetic reflectivity (XRMR) measurements were performed at the Pohang Light Source (beamline 2A). Total electron yield was used for XMCD, while a photodiode was used to record the XRMR data. All measurements were performed at $T \approx 78$ K (liquid-nitrogen), while the magnetization direction was controlled by a 0.2 T electromagnet.

The g -factor of the Co/Cu sample, determined by ferromagnetic resonance (FMR), was found to be 2.48 ± 0.1 ,

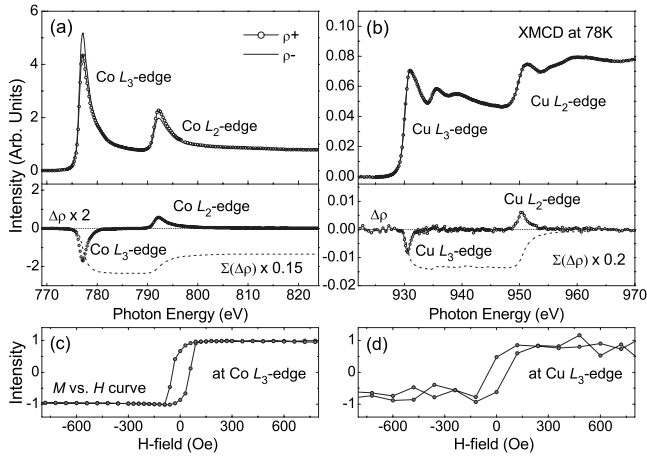


FIG. 1. XMCD results for Co (left) and Cu (right). Upper panels (a, b): absorption spectra, ρ^+ and ρ^- . Middle panels (c) and (d): dichroism signal ($\Delta\rho$) and its integral ($\Sigma(\Delta\rho)$). Bottom panels: M vs H curves measured at maximum $\Delta\rho$.

which is in agreement with a previous result.¹³ The g -factor represents the macroscopic behavior of the magnetic system. In a work, Kittel proposed a simple mean-field-theory formula¹⁴ to relate the macroscopic g -factor, measured by FMR, to the relevant microscopic quantities, viz., the spin- (m_s) and orbital- (m_o) magnetic moments, characterizing a bulk FM material: $(g-2)/2 = m_o/m_s$. These microscopic quantities can be derived element by element from the corresponding absorption spectra taken at the $L_{2,3}$ -edges using circularly polarized incident radiation. The spectra for the magnetization direction parallel and antiparallel to the photon helicity vector (ρ^+ and ρ^-), and the dichroism ($\Delta\rho$) and its integration are displayed in Fig. 1(a). The spectra (ρ_+ and ρ_-), which result from Co $2p \rightarrow 3d$ dipole transitions, are divided roughly into L_3 ($2p_{3/2}$) and L_2 ($2p_{1/2}$) regions. Quantitative estimates, using the sum rule,¹⁷ for both m_s^{Co} and m_o^{Co} give 1.765 and $0.179\mu_B/\text{Co}$ (experimental detail is similar with the previous result¹⁸). These values imply a substantial increase in m_o^{Co} at the interface with the Cu and represents a considerable enhancement ($\sim 12.5\%$) of the moment ratio $m_o^{\text{Co}}/m_s^{\text{Co}} = 0.1016$ over the same ratio in bulk Co. However, using these values in Kittel's formula yields only 2.203 for g^{Co} . Clearly, the ratio enhancement in the FM layer is insufficient per se to explain the observed value of $g = 2.48$.

Due to this discrepancy, it seems probable that some additional contributions might be present. In spin-transfer devices, a fundamental role is played by electronic scattering events at the interface between the magnetic and the non-magnetic materials. These events are indeed capable of modifying the macroscopic magnetic state. In this context, magnetic scattering points in the NM material, such as a magnetic defects and/or impurities, affect the efficiency of spin-flip,^{16,19} thereby modifying the spin-transfer torque. It seems therefore quite appropriate in examining the microscopic origin of the magnetic g -factor, to turn our attention toward the NM Cu layer. The XMCD spectrum at the Cu $L_{2,3}$ is shown in Fig. 1(b). A small but finite dichroism is observed, clearly indicating an induced magnetic polarization in the Cu layer. Moreover, hysteresis curves were recorded at

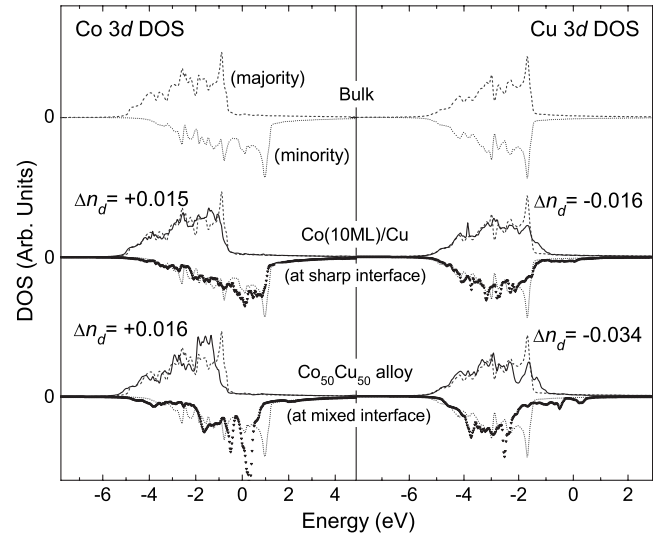


FIG. 2. DOS calculations for $3d$ Co (left panels) and Cu (right panels). Top: bulk Co; bulk Cu. Middle: 10 ML Co on Cu(bulk). Bottom: $\text{Co}_{0.5}\text{Cu}_{0.5}$ alloy. Bulk DOS (light gray) are reproduced in all three panels for comparison.

the maximum of the $\Delta\rho$ at both the Co and the Cu L edges [see, Figs. 1(c) and 1(d)]. The Co and Cu magnetization curves are very similar, indicating a parallel alignment of the Co and Cu moments and a strong coupling between the two magnetizations. Quantitatively, taking into consideration the electron-penetration depth from the dichroism curve of Fig. 1(b), m_s^{Cu} was found to be $0.06\mu_B/\text{Cu}$. On the other hand, it can be seen that the $\Delta\rho$ between Cu L_2 and L_3 edges is nearly identical, indicating an extremely small orbital moment, which is therefore difficult to be reliably deduced from these experimental results. Nevertheless, Cu in the M vs H curve shows a finite coercive field which might be explained either by spin-orbit coupling with Co or by the Cu orbital moment itself.

The interpretation of these results is facilitated by electronic structure calculations. The LMTO band calculations in the local spin density approximation (LSDA) were performed for bulk Co and bulk Cu, for 10 monolayer (ML) Co on bulk Cu as well as for $\text{Co}_{0.5}\text{Cu}_{0.5}$ alloy. These systems were meant to represent an increasing influence of the interface region over the entire system, the bulk (no interface) and the alloy (all interface) being the two extreme cases. Figure 2 shows the $3d$ density of state (DOS) of Co (left panel) and Cu (right panel) compared with the respective bulk DOS. A remarkable trend is captured by the difference in the number of $3d$ electrons, $\Delta n_d = n_d^{\text{film}} - n_d^{\text{bulk}}$. In the Cu interface region Δn_d is negative while Δn_d is positive for the Co, signifying that $3d$ charge is being transferred from Cu $3d$ to Co $3d$ at the interface. Such charge transfer implies the formation of a rather strong bonding of the Co with the Cu, resulting in a broadening of the $3d$ band and a shifting toward a lower energy at the interface. Magnetically, this modification results in calculated induced magnetic moments on Cu of $m_s^{\text{Cu}} = 0.05$ and $m_o^{\text{Cu}} = 0.002\mu_B/\text{Cu}$, which are in very good agreement with the XMCD results.

These microscopic results suggest a crucial role of the

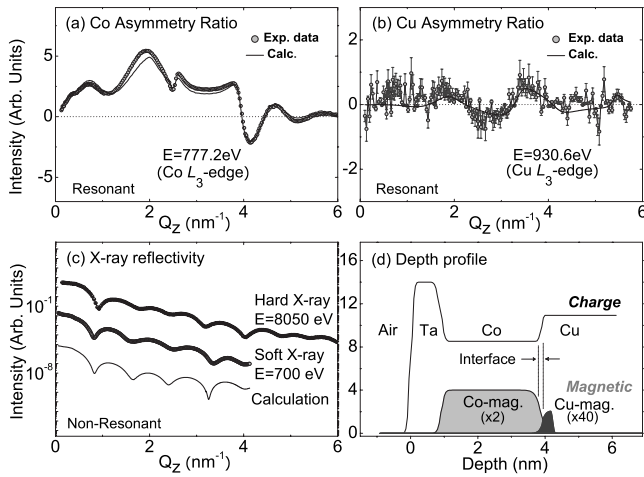


FIG. 3. Asymmetry ratio at the Co (a) and Cu (b) L_3 edges and their calculations. (c) Results of non-resonant x-ray reflectivity, and their calculation. (d) Depth profiles of the density of the charge (line) and the magnetic areas (filled). The dashed lines indicate the Co/Cu interface region.

NM layer in determining the magnetic properties. Since the NM layer carries an induced polarization, it appears reasonable to consider an additional contribution to the g -factor proportional to the induced magnetization. Its distribution can be obtained with great accuracy from XRMR measurements, taken on resonance at the Co and Cu L_3 edge energies.²⁰ Particularly, the magnetic asymmetry ratio (\mathcal{R}) contains a variety of magnetic information, including magnetic thickness, magnetic depth profile, and magnetic moments.²¹ Reflectivity intensities as a function of $Q_z = 4\pi \sin \theta / \lambda$ were measured, point-by-point, for magnetization parallel (I^+) and antiparallel (I^-) to the photon helicity. Here, θ and λ are the scattering angle and the wavelength of the photon, respectively. Figures 3(a) and 3(b) shows the $\mathcal{R} (= \frac{I^+ - I^-}{I^+ + I^-})$ ratio for Co and Cu. Note that although as expected, \mathcal{R} for Co is considerably larger than \mathcal{R} for Cu, the Cu- \mathcal{R} is still well resolved and more importantly it exhibits a line shape quite distinct from the Co one. The magnetic thicknesses on Co and Cu can be obtained from these data reliably. For the calculation of the \mathcal{R} intensity, we used that scattering intensity is simulated by the distorted wave born approximation (DWBA) with the charge and magnetic roughness at the interface.²⁰ The simulation of \mathcal{R} results in estimates of $t_{\text{mag}}^{\text{Co}} = 30$ and $t_{\text{mag}}^{\text{Cu}} = 3.8$ Å. Clearly, the Cu magnetic layer extends over a finite thickness (~ 2 ML), in spite of the extremely small magnetic moments. Additionally, the charge (or structural) profile can be investigated using non-resonant x-ray reflectivity as shown in Fig. 3(c). The charge and magnetic depth-profiles deduced from these data are plotted in Fig. 3(d). The charge profile displays sharp boundaries between the layers, indicating an average roughness of only $\sim 1.0 \pm 0.47$ Å. On the other hand, the magnetic-depth profile is considerably broader. Undoubtedly, the magnetic-depth profile in the Cu layer extends over a finite length.

Considering the finite length of the induced polarization in the NM layer, it seems appropriate to add to the g -factor formula an additional term proportional to $\pm |g^{\text{NM}}|$ and

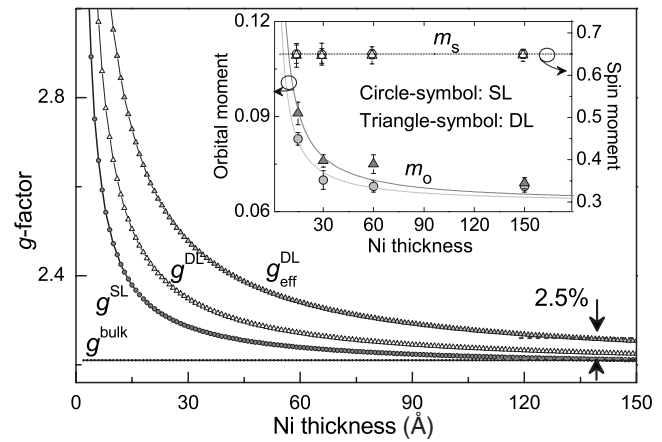


FIG. 4. Calculated g -factors for Ni (SL) and Pd/Ni (DL). g^{DL} and $g_{\text{eff}}^{\text{DL}}$ denote Kittel's model and the model modified by an additional contribution of the Pd layer's weight, respectively. The arrow denotes the enhancement of $g_{\text{eff}}^{\text{DL}}$ in comparison with g^{bulk} . Inset: Ni m_s and m_o for SL and DL. All lines are only guides to the eyes.

weighted by the relative magnetic thicknesses $t_{\text{mag}}^{\text{NM}}/t_{\text{mag}}^{\text{tot}}$.²² Here, g^{NM} can be estimated using the Kittel model and a + (or -) sign would denote ferromagnetic (or antiferromagnetic) coupling between the FM magnetic moments and the induced moment in the NM material. In our case $t_{\text{mag}}^{\text{NM}}/t_{\text{mag}}^{\text{tot}} = 3.8/33.8 = 0.112$ and $g^{\text{NM}} = 2(1 + 0.002/0.06) = 2.06$, giving a positive additive term due to the NM layer of ~ 0.23 . Adding this phenomenological contribution to the Co contribution $g^{\text{Co}} = 2.203$, a total of $g = 2.43$ is finally derived all in terms of microscopic parameters and in excellent agreement with the macroscopic FMR value of 2.48.

The presence of an additional term due to the NM layer in the g -factor formula can be further tested by applying the model to a different system. Particularly, it is interesting to test the model with respect to the magnetic thickness dependence which was estimated. Previous studies on the Pd/Ni bilayer reported an interesting effect: a sizable enhancement of the g -factor (~ 2.3) with respect to a bare Ni layer (2.2) was found even for bilayer systems containing very thick Ni layers.²³ Quite naturally, the role of the NM layer in this enhancement was suspected but no quantitative evidence was offered. Furthermore, the Pd/Ni system is analogous electronically to the Co/Cu system, e.g., charge transfer.¹⁸ The system Pd/Ni was therefore judged appropriate to further extend our g -factor investigation. To exploit the thickness dependence of the g -factor, we fabricated films of several thicknesses. Single Ni layers (SLs), and double Pd(4 Å)/Ni layers (DLs) of variable thickness ($t_{\text{Ni}} = 15, 30, 60,$ and 150 Å) were deposited on a W(110) substrate and their XMCD spectra were measured *in situ* at the Ni $L_{2,3}$ and Pd $M_{2,3}$ edges. The inset in Fig. 4 plots magnetic moments derived from these measurements for the SL and DL (more complete experimental details will be published elsewhere). The most evident effect is the pronounced enhancement of m_o^{Ni} below 60 Å, while the change in m_s (~ 0.65) is negligible. Additionally, the induced Pd moments are found to be $m_s = 0.18$ and $m_o = 0.02 \mu_B/\text{Pd}$, in addition to $t_{\text{mag}}^{\text{Pd}} \approx 4$ Å. This behavior of m_o in DL is especially pronounced because a certain amount of charge is transferred from Pd 4d to Ni 3d

at the interface.¹⁸ This transfer effectively reduces the weight of the Ni $3d^8$ configuration thereby increasing m_o .

The calculated g -factors (g^{SL} and g^{DL}) for SL and DL obtained using Kittel's formula via the findings for both the Ni and the Pd layers are shown in Fig. 4. The additional contribution of the Pd layer was weighted using an induced magnetic thickness, showing $g_{\text{eff}}^{\text{DL}}$. The SL exhibits the conventional $1/t_{\text{Ni}}$ behavior. The $g_{\text{eff}}^{\text{DL}}$ behavior is instead more complicated. Apart from the anomalous $1/t_{\text{Ni}}$ dependence in the thin-film region, there is a small but persistent increase of g even for very thick Ni (2.5% compared to g^{Bulk}). This term is purely due to the NM layer. Clearly this is the term responsible for the increase of the g -factor even for very thick magnetic films noted above. This effect cannot be explained by g^{DL} alone, which is confined in the interface region, but necessitates to take into account the induced polarization of the NM layer. Most importantly, although the induced NM moment is small, its distribution over a layer of finite thickness leads to a further anomalous g -factor term, ultimately affecting the whole system.

In summary, the Landé g -factor behavior has been fully derived, directly and quantitatively, from measured microscopic parameters for two typical FM/NM systems. Particularly relevant is the emergence of the key role played by the NM layer, clearly demonstrating the importance of the distribution of the induced magnetic moment over a layer of finite thickness. We hope that our detailed elucidation of the various microscopic factors influencing the macroscopic behavior of this type of magnetic structure may help in identifying approaches for designing high-quality spintronics.

The NSLS, Brookhaven National Laboratory, is supported by the U.S. DOE, Office of Science, Office of Basic Energy Sciences, under Contract No. DE-AC02-98CH10886. NYU is supported by NSF (Grant No. NSF-DMR-0706322). POSTECH is supported by KRF (Grant No. 2006-312-C00523) and by WCU through KOSEF (Grants No. R31-2008-000-10059-0 and No. R32-2008-000-10180-0). PAL is supported by POSTECH and MOST.

-
- ¹J. A. Katine, F. J. Albert, R. A. Buhrman, E. B. Myers, and D. C. Ralph, *Phys. Rev. Lett.* **84**, 3149 (2000).
²S. I. Kiselev, J. C. Sankey, I. N. Krivorotov, N. C. Emley, R. J. Schoelkopf, R. A. Buhrman, and D. C. Ralph, *Nature (London)* **425**, 380 (2003).
³W. H. Rippard, M. R. Pufall, S. Kaka, S. E. Russek, and T. J. Silva, *Phys. Rev. Lett.* **92**, 027201 (2004).
⁴L. Berger, *Phys. Rev. B* **54**, 9353 (1996).
⁵J. Slonczewski, *J. Magn. Magn. Mater.* **159**, L1 (1996).
⁶F. J. Albert, N. C. Emley, E. B. Myers, D. C. Ralph, and R. A. Buhrman, *Phys. Rev. Lett.* **89**, 226802 (2002).
⁷M. D. Stiles and A. Zangwill, *Phys. Rev. B* **66**, 014407 (2002).
⁸W. Weber, S. Riesen, and H. C. Siegmann, *Science* **291**, 1015 (2001).
⁹R. Urban, G. Woltersdorf, and B. Heinrich, *Phys. Rev. Lett.* **87**, 217204 (2001).
¹⁰Y. Tserkovnyak, A. Brataas, G. E. W. Bauer, and B. I. Halperin, *Rev. Mod. Phys.* **77**, 1375 (2005).
¹¹S. Mizukami, Y. Ando, and T. Miyazaki, *Phys. Rev. B* **66**, 104413 (2002).
¹²S. Mizukami, Y. Ando, and T. Miyazaki, *Jpn. J. Appl. Phys.* **40**, 580 (2001); S. J. Yuan, L. Sun, H. Sang, J. Du, and S. M. Zhou, *Phys. Rev. B* **68**, 134443 (2003).
¹³J.-M. L. Beaujour, J. H. Lee, A. D. Kent, K. Krycka, and C.-C. Kao, *Phys. Rev. B* **74**, 214405 (2006).
¹⁴C. Kittel, *Phys. Rev.* **76**, 743 (1949).
¹⁵A. Brataas, Y. V. Nazarov, and G. E. W. Bauer, *Phys. Rev. Lett.* **84**, 2481 (2000).
¹⁶J. Foros, A. Brataas, Y. Tserkovnyak, and G. E. W. Bauer, *Phys. Rev. Lett.* **95**, 016601 (2005).
¹⁷B. T. Thole, P. Carra, F. Sette, and G. van der Laan, *Phys. Rev. Lett.* **68**, 1943 (1992); C. T. Chen, Y. U. Idzerda, H.-J. Lin, N. V. Smith, G. Meigs, E. Chaban, G. H. Ho, E. Pellegrin, and F. Sette, *ibid.* **75**, 152 (1995).
¹⁸J.-S. Lee, J.-Y. Kim, J. H. Shim, B. I. Min, K.-B. Lee, and J.-H. Park, *Phys. Rev. B* **76**, 060403(R) (2007).
¹⁹J. B. Johnson, *Phys. Rev.* **32**, 97 (1928); H. Nyquist, *ibid.* **32**, 110 (1928).
²⁰D. R. Lee, S. K. Sinha, D. Haskel, Y. Choi, J. C. Lang, S. A. Stepanov, and G. Srajer, *Phys. Rev. B* **68**, 224409 (2003).
²¹C. C. Kao, C. T. Chen, E. D. Johnson, J. B. Hastings, H. J. Lin, G. H. Ho, G. Meigs, J.-M. Brot, S. L. Hulbert, Y. U. Idzerda, and C. Vettier, *Phys. Rev. B* **50**, 9599 (1994).
²²The additional term is set up ad hoc for a NM-FM system. If a NM layer is not magnetically polarized, this term can be ignored.
²³J. C. Gonzalez-Pons, J. J. Henderson, E. del Barco, and B. Ozyilmaz, *Phys. Rev. B* **78**, 012408 (2008).